NANO LETTERS

2007
Vol. 7, No. 12
3734−3738

Ordered Vacancy Compounds and Nanotube Formation in $CuInSe_2$–CdS Core–Shell Nanowires

Hailin Peng,[†] Chong Xie,[†] David T. Schoen,[†] Kevin McIlwrath,[‡] Xiao Feng Zhang,[‡] and Yi Cui*,[†]

Department of Materials Science and Engineering, Stanford University, Stanford, California 94305, and Electron Microscope Division, Hitachi High Technologies America, Inc., 5100 Franklin Drive, Pleasanton, California 94588

Received August 24, 2007; Revised Manuscript Received October 15, 2007

ABSTRACT

$CuInSe_2$ related materials-based heterojunction diodes have received much attention, owing to their highest power conversion efficiency (19.5%) among all the thin-film solar cell technologies. Important issues on the microstructure and formation mechanism of $CuInSe_2$–CdS p-n heterojunction persist due to the complexity of polycrystalline films and invasive sample preparation for characterization. Here, we investigated the microstructure, chemical composition, and formation mechanism of the junction with $CuInSe_2$–CdS core–shell nanowires, where nanowire geometry affords single-crystalline nanograins for direct characterization. A coherent CdS shell can be epitaxially deposited onto the $CuInSe_2$ nanowire with chemical bath deposition even at 60 °C. For the first time, ordered vacancy compound nanodomains induced by fast outward diffusion of Cu ions were directly observed near the interface of epitaxial CIS–CdS heterostructure. The core–shell nanowires can be transformed into nanotubes with chemical bath deposition progression through a nanoscale Kirkendall effect. Our results provide important understanding of $CuInSe_2$–CdS heterojunctions for developing better $CuInSe_2$ solar cells.

$CuInSe_2$ (CIS) related materials have the highest power conversion efficiency (19.5%) among all the thin-film solar cell technologies.[1,2] CIS is a direct-band gap chalcopyrite semiconductor with high optical absorption coefficients ($>10^5$ cm^{-1}) and is used as a photon absorber in thin-film solar cells.[3] CIS is commonly paired with CdS to form the p-n heterojunction that separates the photogenerated electron−hole pairs.[4] The interface between CIS and CdS is of key importance to the performance of the solar cell device.[3] It has been speculated that a distinct Cu-deficient n-type layer, an ordered vacancy compound (OVC), is formed at the surface layer of the p-type CIS film next to the weakly n-type CdS buffer layer and causes large band bending that contributes to device performance.[5,6] However, so far there is no conclusive evidence concerning the actual structure and formation mechanism of OVC because OVC has not been observed directly at the CIS−CdS interface.[7,8] Previous transmission electron microscopy (TEM) studies have specifically looked at the interfacial region of cross-section thin-film sample,[7−9] which are often prepared by high-energy Ar ion-beam milling. However, it was pointed out that artifacts and changes in microstructure and composition of the interface produced by Ar ion-beam milling are unavoidable, even when the milling is carefully operated at low-sputtering ion energy (0.5 keV) and small inclination angle (7°).[10] It is extremely difficult to accurately determine the structure and formation mechanism of the heterojunctions of polycrystalline film samples.

Recently, we developed CIS nanowires (NWs) as novel photovoltaic materials.[11] NWs afford single-crystalline nanograins for direct characterization. In contrast to thin film studies, the CIS−CdS core−shell heterojunction NW geometry can provide identifiable microstructure and composition for directly investigating the heterojunction formation by high-resolution TEM and energy dispersive X-ray spectrometry (EDX) analysis without invasive TEM sample preparation. Here, we studied the junction with CIS−CdS core−shell NWs. A coherent CdS shell can be epitaxially deposited onto the CIS NW with chemical bath deposition (CBD) even at 60 °C. For the first time, an OVC was directly observed at the CIS−CdS junction and was shown to exist in nanoscale domains. Remarkably, the core−shell NWs can be transformed into nanotubes with CBD progression through a nanoscale Kirkendall effect.[12,13] Our results provide important guidelines for better CIS solar cells.

We have shown that single-crystal CIS NWs could be synthesized by Au nanoparticle-catalyzed vapor−liquid−solid growth (See Supporting Information).[11] CIS NWs with

* To whom correspondence should be addressed. E-mail: yicui@stanford.edu.
[†] Stanford University.
[‡] Hitachi High Technologies America, Inc.

10.1021/nl0721463 CCC: $37.00
Published on Web 11/13/2007

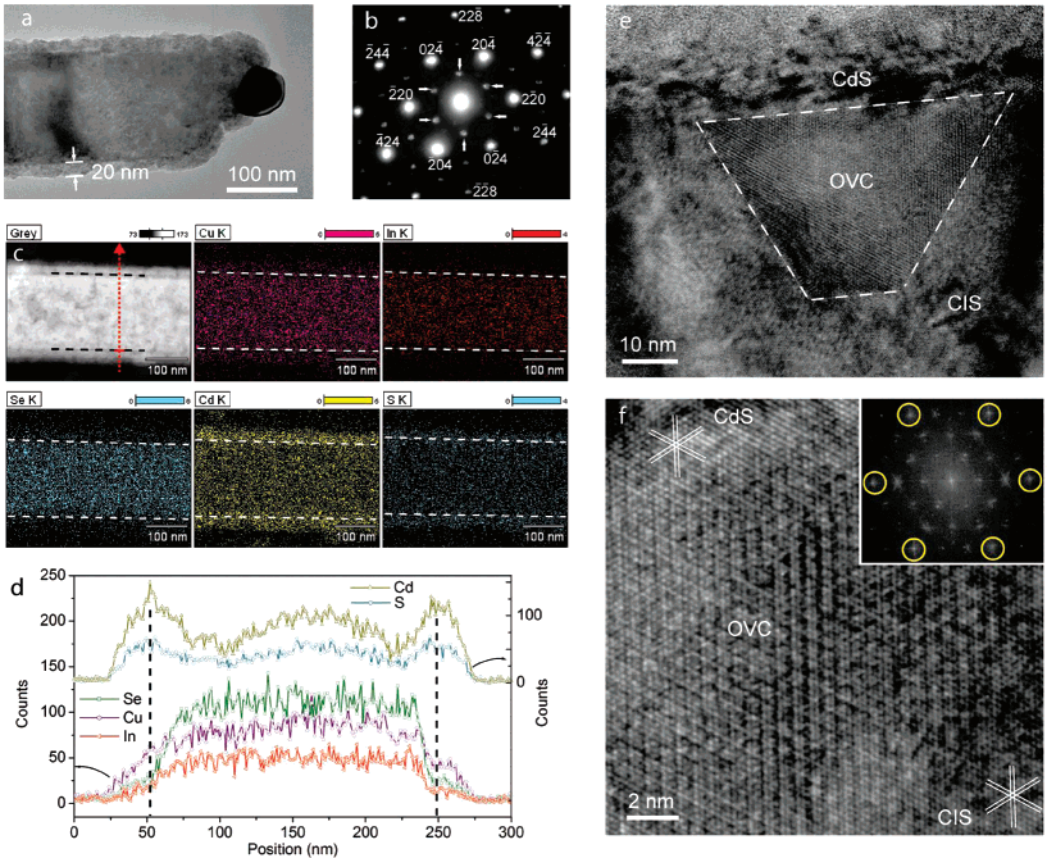

Figure 1. Microstructure and composition of the CIS−CdS core−shell NW after 5 min CBD. (a,b) TEM image and corresponding SAED pattern. (c) STEM image and corresponding EDX elemental mapping of Cu, In, Se, Cd, and S. (d) EDX line-scanning across the NW diameter indicated by a red line in panel c. The black dashed lines show the CdS/CIS interface. (e) TEM image showing the superstructure domain in the interface region of CdS/CIS. (f) HRTEM image showing the lattice spacing of 0.206 nm and the corresponding FFT image (inset). The spots in the yellow cycles are indexes as the (220) family of lattice planes in $CuIn_5Se_8$ taken along the [221] zone axis.

a stoichiometry of nearly 1:1:2 have a regular chalcopyrite structure with a growth direction along the [1-10] direction while Cu-deficient CIS NWs with a stoichiometry of 1:2.3:3.4 have the same growth direction but with a superlattice structure presumably formed by vacancy ordering.[11] Here, we use only regular 1:1:2 CIS NWs for the studies, which is close to the composition of CIS films in solar cells. CIS−CdS core−shell heterostructured NWs were prepared by growing a thin CdS layer at the surfaces of CIS NWs via CBD at 60 °C, which are the conditions typically used in thin film solar cell fabrication (See Supporting Information).[2]

A bright-field TEM image shows that the core−shell NW has a 19−23 nm thick coherent shell after 5 min CBD (Figure 1a). The selected area electron diffraction (SAED) pattern (Figure 1b) can be indexed as taken along the [221] zone axis of CIS. The regular spots in SAED suggest the epitaxial orientation relationship between the CIS core and the CdS shell. That is, the CIS−CdS core−shell NWs are single-crystalline. This is consistent with the well-established epitaxial relationship on planar structures.[14] It was found that thin CdS films can be epitaxially grown on both [112]- and [100]-orientated CIS substrates with predominantly the cubic CdS structure using suitable solution composition at 60 °C.[14] CIS has a tetragonal structure with $a = 0.578$ nm and $c = 11.62$ nm, which can be effectively considered as stacking two cubic cells along the c-axis. The lattice parameters have an excellent match with cubic CdS ($a = 0.582$ nm, $\Delta a/a = 0.7\%$). The six bright diffraction spots arranged in a hexagonal symmetry correspond to the (220) family of lattice planes in CIS and the (220) family in cubic CdS. As shown in Figure 1b, extra weak diffraction spots indicated by arrowheads are indexed as the (424)/3 family of CIS lattice planes, which are forbidden in regular 1:1:2 CIS compound and NW.[11] Their appearance results from the planar defects.[15−17]

One important question is whether the ions can diffuse around during the 5 min CBD process, which can cause defect formation. Spatially resolved EDX measurements have been carried out to map the chemical composition of core−shell NWs with 1.2 nm resolution. Figure 1c shows the scanning TEM (STEM) image of a CIS−CdS core−shell NW and the false color images of its elemental distribution. The dashed lines indicate the interface position of CIS−CdS determined with STEM image. The EDX mapping in Figure 1c indicates a significant outward diffusion of Cu while little diffusion of In and Se. Cd and S are mostly distributed in the shell although it not possible to determine whether Cd and S go into the CIS core in the horizontal NW geometry because the shell surrounds the whole NW. A clear presentation of the elemental distribution is given by a plot of the EDX line-scanning signal versus the distance across the NW diameter. The red line on the TEM image shown in Figure

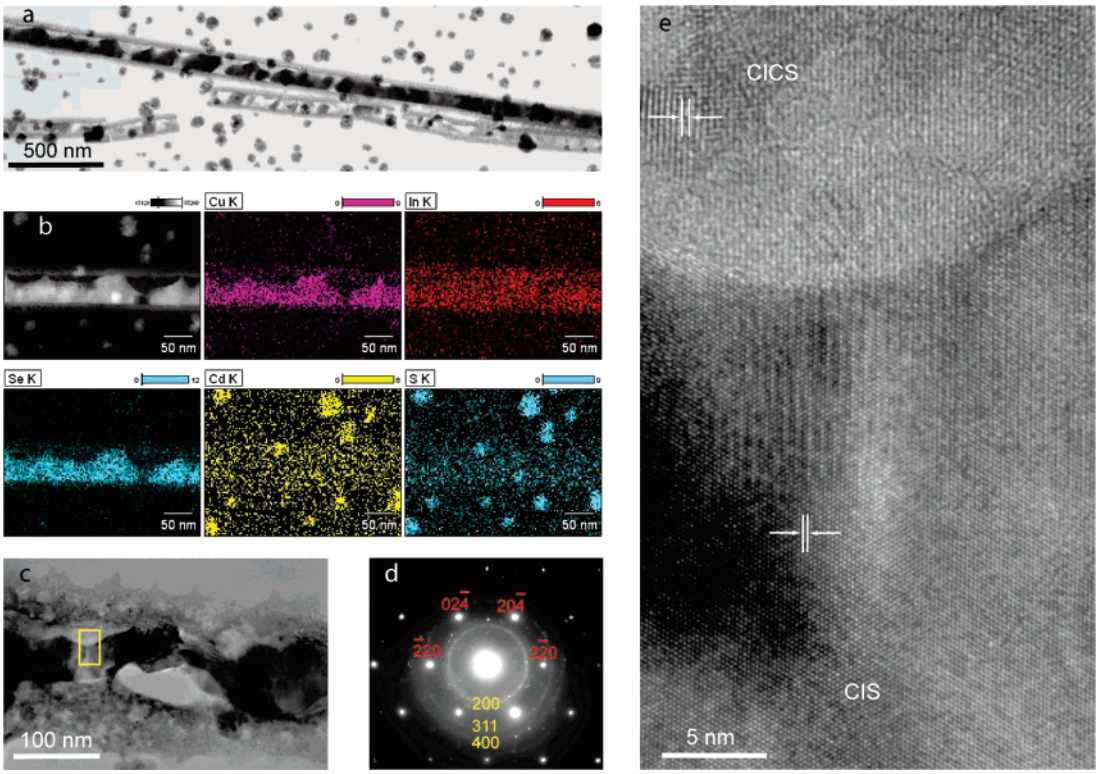

Figure 2. Formation of voids after 12 min CBD. (a) TEM image of nanotubes with remaining core CIS, showing the random-sized Kirkendall voids distributed at the interface. (b) EDX elemental mapping of Cu, In, Se, Cd, and S. (c) Close-up view of the voids in panel a. (d) Corresponding SAED pattern. (e) Atomic-resolution TEM image recorded from the yellow boxed area in panel c showing the lattice spacing of 0.206 nm in CIS core and 0.290 nm in CICS shell. The Kirkendall diffusion leads to voids formed at the interface of remaining CIS and CICS shell.

1c indicates the path of electron beam scanning. It is evident from Figure 1d that Cu signals (purple) are present in the CdS layer. On the basis of these data, we think that Cu ions are the main species diffusing during the 5 min CIS−CdS interface formation. This is reasonable because Cu ions have a relatively high chemical diffusion rate and ionic conductivity in the chalcopyrite materials[18−20] and is also consistent with previous OVC studies.[8]

The second important question is whether the OVC forms at the CIS−CdS NW interface and what structure it has. TEM images show the existence of a 1250 nm^2 trapeziform OVC nanodomain of CIS structures at the CIS−CdS interface although other shapes of OVC domains also exist (Figure 1e). An HRTEM micrograph recorded near the interfacial region clearly reveals the (3 × 3) periodicity superlattice structure within the nanodomains, characteristic of the proposed OVC structure (Figure 1f).[21] The OVC nanodomains have an epitaxial relationship with the CIS core and CdS shell. Superlattice structure exists along three directions, consisting of high-density Cu vacancies laying on [1-10], [10-2], and [01-2] planes. The fast Fourier transform (FFT) of the real-space image can be identified as the diffraction pattern from the [221] zone of a $CuIn_5Se_8$ OVC structure ($a = 4.040 \pm 0.005$ Å and $c = 32.75 \pm 0.02$ Å).[21] The number density of OVC domain is about 10 per micrometer length. We emphasize that this is the first time OVC is observed directly at the CIS−CdS interface, and we experimentally prove its structure.

Another important question is whether the Cu ions keep diffusing out of the CIS NW core and whether there is a structure change after a longer CBD. To investigate that, we have extended the CBD time to 12 and 16 min, which is typical for thin film CIS solar cell fabrication.[2] After 12 min CBD, random-sized nanoscale voids were observed at the CIS/CdS interface (Figure 2a). Both isolated grains and continuous core imbedded in the shell are observed. Energy dispersive spectrometry mapping data confirm the existence of the elements Cu, In, Se in the remaining core materials (Figure 2b). Compared to the sample with only 5 min CBD, in which only the Cu diffusion is significant, NWs with 12 min CBD show that not only Cu but also In and Se diffuse into the CdS shell and even onto the carbon-supporting film. The elemental EDX signal strengths of Cd and S at 12 min CBD show no contrast between the core and shell, suggesting inward diffusion of Cd and S. We think that supersaturated vacancies can condense to form small holes in the shell (see Supporting Information, Figure S1). Detailed TEM and SAED analysis reveal that the shell now becomes polycrystalline, but the remaining core grains remain textured (Figure 2c,d). The SAED pattern (Figure 2d) shows the hexagonal spots pattern for CIS crystalline core with chalcopyrite structure, but weak spotty rings from the polycrystalline shell can also be observed. Three diffraction rings can be indexed as (200), (311), (400) planes of cubic phase $CuInCdSe_2S$ (CICS, F-43 m, $a = 5.803$ Å, JCPDS no. 00−056-1195), respectively.[22] The HRTEM image

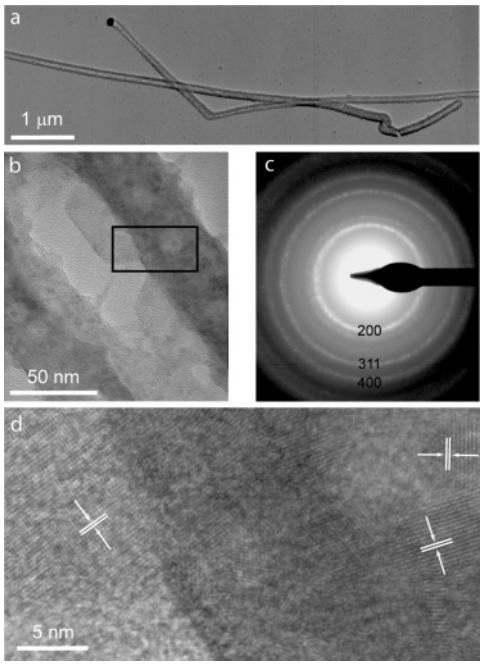

Figure 3. Formation of nanotubes after 16 min CBD. (a) TEM image of nanotubes. (b) Close-up view of the wall of nanotube in panel a. (c) Corresponding SAED pattern of the nanotube, showing the polycrystalline structures and voids in the wall. (d) HRTEM of a wall of the tube (recorded from boxed area in panel b) showing the lattice spacing of 0.290 nm.

shows single-crystalline CIS grains imbedded in the polycrystalline CICS shell (Figure 2e).

As the CBD reaction proceeds to 16 min, the CIS cores completely disappear, leading to the formation of nanotubes. A TEM image (Figure 3a) shows that two nanotubes can be clearly identified. The coating of the CdS layer is conformal during the CBD process so that a zigzag CIS wire results in a kinked tube and the Au nanoparticle catalyst is encapsulated in the tube. EDX analysis indicates that the nanotubes are composed of Cu, In, Se, Cd and S and there is also some amount of oxygen incoporation (see Supporting Information, Figure S2). The elemental distribution is quite uniform along the tube. A high magnification image of a nanotube shows the presence of small voids and cracks in the nanotube wall (Figure 3b). The thickness of the wall is about 40 nm. The SAED pattern of the nanotube shows spotty rings representative of a polycrystalline sample. As shown in Figure 3c, these features can be assigned to the (200), (311), (400) planes of cubic phase CICS.[22] An HRTEM image near a tube-wall region (Figure 3d) reveals the random arrangement of crystalline nanograins. Lattice fringes with a spacing of 0.290 nm are visible in these nanograins, which is in good agreement with the spacing of (200) planes of cubic CICS.

The structure evolution of CIS−CdS core−shell NWs has characteristics reminiscent of the nanoscale Kirkendall effect. The Kirkendall effect describes void formation due to the difference of species diffusivity during alloying or solid chemical reaction.[23−25] The nanoscale Kirkendall effect was discovered recently during the formation of hollow cobalt sulfides and oxides by cobalt nanocrystal sulfidation

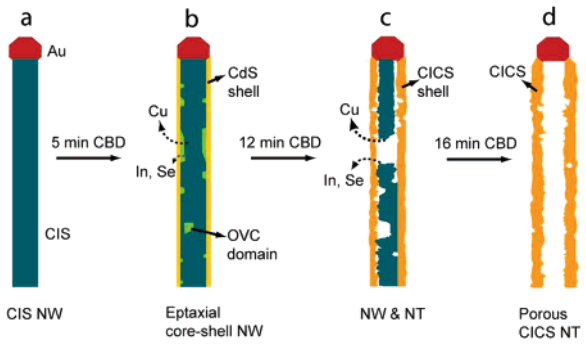

Figure 4. Schematic diagram of the formation process of CIS−CdS core−shell nanowires and nanotubes. (a) Single-crystal CIS nanowires are grown by the vapor−liquid−solid mechanism using Au nanoparticles as a catalyst. (b) The nanowires are coated with a thin CdS layer via 5 min CBD at 60 °C, forming core−shell CIS−CdS epitaxial nanowires. OVC nanodomains (green) form at the CIS−CdS interface mainly due to Cu fast outward diffusion. (c) The 12 min CBD leads to the formation of nanoscale voids by the nanoscale Kirkendall effect. The shell composition becomes CICS (orange). (d) Polycrystalline CICS nanotube forms after 16 min CBD.

and oxidation, respectively.[12,26] The effect has been further explored in the synthesis of other hollow nanocrystals[27] and $ZnAl_2O_4$ nanotubes.[13,28] Now let us look at the key characteristics during the CBD of CdS onto CIS NWs (Figure 4). (1) Ion diffusion: Cu ions have a large diffusion coefficient in CIS and CdS. In the initial stage of CBD, Cu ions are the main diffusing species and activate the CIS and CdS lattice by forming a large concentration of vacancies. In the later stage of CBD, In, Se, Cd, and S ions can also diffuse due to the activation effect. (2) Vacancy dynamics: The increased concentrations of vacancies in CIS first self-organize to form the OVC superlattice structure at the CIS−CdS interface. The superlattice structure is unique for CIS materials and has not been observed in previous hollow nanostructures formed by Kirkendall effect[12,26] The OVC exists in the form of multiple nanodomains instead of only one domain because the size of CIS NW is still large compared to the size of single domains. The further increase of vacancy concentration results in supersaturation, and vacancies condense to form voids and eventually nanotubes, analagous to $ZnAl_2O_4$ nanotube formation.[13] (3) The shell changes from initial epitaxial single-crystalline CdS to polycrystalline and porous CICS due to dramatic ion diffusion and vacancy dynamics in the shell. And the low temperature (60 °C) of CBD process is not high enough to anneal the nanotube to form single crystal.

In summary, we have investigated the microstructure, chemical composition, and formation mechanism of CIS−CdS core−shell heterojunction NWs. Fast outward diffusion of Cu favors the formation of OVC nanodomains near the interface of epitaxial CIS−CdS heterostructure. OVC has the $CuIn_5Se_8$ structure. Diffusion processes lead to the formation of voids and CICS nanotubes through the nanoscale Kirkendall effect. Our results provide important understanding of CIS−CdS heterojunctions for developing better CIS solar cells.

Acknowledgment. Y.C. acknowledges support from Stanford New Faculty Startup Fund, GCEP, CPN, and CIS. D.T.S. acknowledges support from NDSEG Fellowship.

Supporting Information Available: Experimental methods and materials, TEM image, and EDX spectra of $CuInSe_2$−CdS NTs. This material is available free of charge via the Internet at http://pubs.acs.org.

References

(1) Green, M. A.; Emery, K.; King, D. L.; Hishikawa, Y.; Warta, W. *Prog. Photovolt: Res. Appl.* **2007**, *15*, 35−40.
(2) Ramanathan, K.; Contreras, M. A.; Perkins, C. L.; Asher, S.; Hasoon, F. S.; Keane, J.; Young, D.; Romero, M.; Metzger, W.; Noufi, R.; Ward, J.; Duda, A. *Prog. Photovolt: Res. Appl.* **2003**, *11*, 225−230.
(3) Beach, J. D.; McCandless, B. E. *MRS Bulletin* **2007**, *32*, 225.
(4) Rockett, A.; Birkmire, R. W. *J. Appl. Phys.* **1991**, *70*, R81−R97.
(5) Schmid, D.; Ruckh, M.; Grunwald, F.; Schock, H. W. *J. Appl. Phys.* **1993**, *73*, 2902−2909.
(6) Kronik, L.; Burstein, L.; Leibovitch, M.; Shapira, Y.; Gal, D.; Moons, E.; Beier, J.; Hodes, G.; Cahen, D.; Hariskos, D.; Klenk, R.; Schock, H.-W. *Appl. Phys. Lett.* **1995**, *67*, 1405−1407.
(7) Nakada, T. *Thin Solid Films* **2000**, *361*−*362*, 346−352.
(8) Abou-Ras, D.; Kostorz, G.; Romeo, A.; Rudmann, D.; Tiwari, A. N. *Thin Solid Films* **2005**, *480*−*481*, 118−123.
(9) Wu, Y. R. F.; Yang, P. *Nano Lett.* **2002**, *2*, 83−86.
(10) Yan, Y.; Jones, K. M.; Noufi, R.; Al-Jassim, M. M. *Thin Solid Films* **2007**, *515*, 4681.
(11) Peng, H.; Schoen, D. T.; Meister, S.; Zhang, X. F.; Cui, Y. *J. Am. Chem. Soc.* **2007**, *129*, 34−35.
(12) Yin, Y.; Rioux, R. M.; Erdonmez, C. K.; Hughes, S.; Somorjai, G. A.; Alivisatos, A. P. *Science* **2004**, *304*, 711−714.
(13) Fan, H. J.; Knez, M.; Scholz, R.; Nielsch, K.; Pippel, E.; Hesse, D.; Zacharias, M.; Gösele, U. *Nat. Mater.* **2006**, 5, 627−631.
(14) Furlong, M. J.; Froment, M.; Bernard, M. C.; Cortes R.; Tiwari, A. N.; Krejci, M.; Zogg, H.; Lincot, D. *J. Cryst. Growth* **1998**, *193*, 114−122.
(15) Lauhon, L. J.; Gudiksen, M. S.; Wang, D. L.; Lieber, C. M. *Science* **2002**, *420*, 57−61.
(16) Xiao, H. Z.; Yang, L.-C.; Rockett, A. *J. Appl. Phys.* **1994**, *76*, 1503−1510.
(17) Xiao, H. Z.; Daykin, A. C. *Ultramicroscopy* **1994**, *53*, 325−331.
(18) Dagan, G.; Ciszek, T.; Cahen, D. *J. Phys. Chem.* **1992**, *96*, 11009−11017.
(19) Gartsman, K.; Chernyak, L.; Lyahovitskaya, V.; Cahen, D.; Didik, V.; Kozlovsky, V.; Malkovich, R.; Skoryatina, E.; Usacheva, V. *J. Appl. Phys.* **1997**, *82*, 4282−4285.
(20) Fuhrmann, B. H. S. L.; Höche, H.-R.; Schubert, L.; Werner, P.; Gösele, U. *Nano Lett.* **2005**, *5*, 2524−2527.
(21) Tham, A.-T.; Su, D. S.; Neumann, W.; Schubert-Bischoff, P.; Beilharz, C.; Benz, K. W. *Cryst. Res. Technol.* **2001**, *36*, 303−308.
(22) Zmii, O. Volyn State University, Lutsk, Ukraine. ICDD Grant-in-Aid, 2004.
(23) Kirkendall, E. O. *Trans. AIME* **1942**, *147*, 104−110.
(24) Smigelskas, A. D.; Kirkendall, E. O. *Trans. AIME* **1947**, *171*, 130−142.
(25) Nakajima, H. *J. Miner. Met. Mater. Soc.* **1997**, *49*, 15−19.
(26) Yin, Y.; Erdonmez, C. K.; Cabot, A.; Hughes, S.; Alivisatos, A. P. *Adv. Funct. Mater.* **2006**, *16*, 1389−1399.
(27) Wang, Y. L.; Cai, L.; Xia, Y. N. *Adv. Mater.* **2005**, *17*, 473−477.
(28) Pijpers, J. J. H.; E. H.; Milder, M. T. W.; Fanciulli, R.; Savolainen, J.; Herek, J. L.; Vanmaekelbergh, D.; Ruhman, S.; Mocatta, D.; Oron, D.; Aharoni, A.; Banin, U.; Bonn, M. *J. Phys. Chem. C* **2007**, *111*, 4146−4152.

NL0721463